

# Extended Bose-Hubbard model with incompressible states at fractional numbers

H. Heiselberg\*

*Danish Defense Research Establishment, Ryvangsalle' 1, DK-2100 Copenhagen Ø, Denmark*

The Bose-Hubbard model is extended to include nearest and far neighbor interactions and is related to the fractional quantum Hall effect (FQHE). Both models may be studied in optical lattices with quantum gases. The ground state is calculated for the extended Bose-Hubbard model with strong repulsive interactions (weak hopping). Incompressible Mott insulator states are found at rational filling fractions compatible with the principal and secondary FQHE filling fractions of the lowest Landau levels observed experimentally. It is discussed to which extent these states at fractional filling survive or undergoes a Mott insulator transition to a superfluid as hopping terms are included.

PACS numbers: 03.75.Hh, 73.43.-f, 71.10.-w, 03.75.Lm

## I. INTRODUCTION

Quantum gases provide new insight in strongly correlated quantum systems and phase transitions in systems of interacting bosons and fermions. A variety of interesting phases exist in various dimensions such as superfluids, Mott insulators, charge density waves, incompressible states in the integer and fractional quantum Hall effect (FQHE) [1, 2, 3, 4, 5], etc. Lattices appear naturally in solids and spin models [6, 7, 8, 9], and recently also optical lattices with Bose atoms have been studied [11, 12]. The superfluid to Mott insulator transition has been observed [13] as predicted from the Bose-Hubbard model. It has been suggested [14] that by applying an additional magnetic field the optical lattices provide a clean system without impurities, where the FQHE can be studied in detail. Alternatively, rapidly rotated harmonic oscillator traps with cold Fermi or Bose atoms may also form a 2D Hall fluid [15, 16, 17].

These possibilities stimulate renewed interest in the long standing problem of the FQHE and its numerous incompressible quantum liquid states at mysterious filling fractions of the lowest Landau levels [1, 2]. In a recent experiment [3] new FQHE fractions are found at  $3/8$ ,  $4/11$ ,  $5/13$ ,  $6/17$ ,  $7/11$ , etc., which fall outside the Laughlin fractions  $1/(2m+1)$  and Jain fractions  $m/(2m \pm 1)$  for integer  $m$ .

The Hubbard model is widely used to describe a number of systems such as strongly correlated electrons. Quantum gases of Bose atoms in optical lattices have recently been described by the Bose-Hubbard model, which in one dimension reads

$$H_{BH} = \sum_i t_1 (b_i^\dagger b_{i+1} + b_{i+1}^\dagger b_i) + U_0 n_i (n_i - 1). \quad (1)$$

Here,  $t_1$  is the hopping parameter to nearest site and  $U_0$  is the on-site interaction energy. The system is a superfluid except in the cases where the filling fraction is

precisely an integer and the hopping term is sufficiently small, where a transition occurs from a superfluid to a Mott insulator as observed in [13]. Including nearest neighbor interaction leads to charge density waves and crystalline structure at half filling and a related Mott transition [17, 18, 19].

We shall be interested in extended Bose-Hubbard models (EBHM) including not only on-site interactions  $U_0$  but also interactions  $U_n$  between particles  $n = 1, 2, 3, 4, \dots$  sites away. In the strongly interacting (atomic) limit or equivalently weak hopping,  $t_1 \ll U_n$ , the extended Bose and Fermi Hubbard models reduce to well known spin models. The Ising model [6] has only nearest neighbor  $U_1$  interactions but next-nearest neighbor interactions  $U_2$  have also been included (see, e.g., [8, 9]).

The purpose of this work is to point to a connection between the Hamiltonian for the FQHE and the EBHM as outlined in section II. Subsequently in section III to find the ground state of the EBHM in the strongly interacting limit, calculate its energy, chemical potential, pressure, etc. Most importantly, a spectrum of incompressible Mott insulator states are found whenever the filling fraction is a rational number  $q/n$ . In section IV the Bose filling fractions are related to the fermion FQHE case, and it is shown that they contain the Laughlin and Jain sequences [2, 20] as well as all the secondary FQHE fractions found experimentally [3]. Finally in section V the effect of hopping terms and the survival of Mott insulator states at fractional filling is discussed.

## II. APPROXIMATING THE FQHE AS AN EXTENDED BOSE-HUBBARD MODEL

The fractional quantum Hall systems [5] can be essentially reduced to the problem of  $N$  spinless electrons with repulsive interactions in  $M$  available states [22]. In the disk geometry the states are  $\psi_k(z) = z^k \exp(-|z|^2/4)/\sqrt{2\pi 2^k k!}$ ,  $k = 0, 1, \dots, M-1$ ;  $z = x + iy = re^{i\phi}$  in units of the magnetic length  $l$  [21].

When the filling fraction is exactly  $\nu = N/M = 1$ ,  $1/3$ ,  $1/5$ ,  $1/7$ , etc., the ground state is the antisymmetric

---

\*Also at Univ. of S.Denmark; Electronic address: hh@ddre.dk

Laughlin wave function

$$\Psi_m = A \prod_{i < j}^N (z_i - z_j)^m \exp \left( - \sum_k^N |z_k|^2 / 4 \right), \quad (2)$$

with  $m = 1, 3, 5, 7$ , etc., and normalization factor  $A^2$ . Analogously, a symmetric Laughlin wave function with  $m = 2, 4, 6, \dots$  can be separated for bosons instead of fermions.

In the lowest Landau level ( $N \leq M$ ) the total wave function also contains a symmetric part  $\Psi_S$

$$\Psi = \Psi_S(z_1, \dots, z_N) \Psi_m. \quad (3)$$

The remaining FQHE problem is to find the incompressible states of  $\Psi_S$  besides the fractions  $\nu = 1, 1/3, 1/5, \dots$  implicit in the Laughlin wave function. At these fractions  $\Psi_S = 1$ .

In the following we shall concentrate on the lowest Landau level,  $N \leq M$ , and study the symmetric wave function  $\Psi_S$  for  $N$  particles in  $M_B = M - mN$  available states. Here the number of states, that the Laughlin wave function use up, have been subtracted. By this “bosonization” the  $N$  particles has thus become  $N$  spinless bosons in  $M_B$  states with a symmetric many-boson wave function  $\Psi_S$  (see, e.g. [23] for details on bosonization). The Bose filling fraction  $\nu_B = N/M_B$  is related to the fermion one by

$$\nu = \frac{N}{M} = \frac{\nu_B}{1 + m\nu_B}, \quad (4)$$

with  $m = 1, 3, 5, \dots$

We can choose any other orthogonal basis from  $\psi_k(z)$ . This may be convenient if a many-body wave function can be constructed from this new basis such that the Hamiltonian approximately diagonalizes. This would greatly simplify the search for the ground state of the FQHE. A candidate for such a convenient basis are the localized Wannier-type wave functions

$$\Phi_j(z) = \frac{1}{\sqrt{2\pi M_B}} \sum_{k=0}^{M_B-1} \psi_k(z) e^{-i2\pi k j / M_B}. \quad (5)$$

where  $j = 0, 1, \dots, M_B - 1$ . As described in Appendix A these wave functions are localized in angle  $\phi$  around  $2\pi j / M_B$ .

Dyakonov argues in Ref. [22] the similar localized wave functions are useful for constructing a crystal-like many-body state that contains at least some of the right features of the FQHE ground state. The localized wave functions of Ref. [22] are an approximate model for the FQHE on a circle. It is simple and illustrative, and is therefore described in Appendix A.

It should be emphasized that the localized states are simply another basis. They are not generated by an external periodic potential as, e.g., an atomic lattice. Whether the basis is “better” will depend on whether

the repulsion between particles dominates over hopping leading to localized vs. conduction states respectively. It will be argued below that localized states of Eq. (5) may be the preferred ones.

The Hamiltonian in the lowest Landau level is now a one dimensional lattice model containing only repulsive two-body interaction  $V$  between the particles

$$H = \sum_{1 \leq i < j \leq N} V(z_i - z_j). \quad (6)$$

The interactions can in the following be almost any repulsive potential including the standard Coulomb:  $V = e^2/|z_1 - z_2|$ . The delta function potential should be treated with care as discussed in Appendix A.

The kinetic energies and other degrees of freedom are absorbed in the cyclotron energies,  $\hbar\omega_c = eB/mc$ , of the lowest Landau level. The cyclotron energies have been subtracted so that only interaction energies remain in the Hamiltonian. In this sense the system is strongly interacting. All energies of this Hamiltonian will scale with the overall strength of the two-body potential.

In tight-binding models the interaction is often written in second quantized form as

$$H = \frac{1}{2} \sum_{ij, i'j'} V_{ij, i'j'} b_i^\dagger b_j^\dagger b_{i'} b_{j'}, \quad (7)$$

where  $b_i^\dagger$  is the usual creation operator of a state  $\Phi_i$  at site  $i$ , and

$$V_{ij, i'j'} = \int \Phi_i(z_1) \Phi_j(z_2) \Phi_{i'}^*(z_1) \Phi_{j'}^*(z_2) |\Psi_m(z_1, z_2, \dots)|^2 V(z_1 - z_2) dz_1 dz_2, \quad (8)$$

are the four-center integrals. Here, the Laughlin wave function present in the total wave function is included in which all other particles have been integrated out.  $|\Psi_m|^2$  does not affect the integrals much except that it contains a correlation hole  $\sim (z_1 - z_2)^{2m}$  which screens short distances of the two-body interaction.

The largest of the  $V_{ij, i'j'}$  are the interaction between particles on just two sites, the direct  $i = i', j = j'$  and the exchange  $i = j', j = i'$ . As described in Appendix A the other overlap integrals are small because the localized wave functions are rapidly oscillation in angle and interfere destructively. We therefore extract the largest (tight binding) direct and exchange part of the FQHE Hamiltonian of Eq. (7)

$$H_0 = \frac{1}{2} \sum_{ij, ij} (V_{ij, ij} + V_{ij, ji}) n_i [n_j - \delta_{i,j}]. \quad (9)$$

Here,  $n_i = b_i^\dagger b_i$  is the number operator on site  $i$ .

For long range interactions such that the two-body interaction can be treated as a constant,  $V \simeq V_0$ , only the direct interaction survives, i.e.  $V_{ij, i'j'} = V_0 \delta_{i, i'} \delta_{j, j'}$ , and therefore  $H = H_0$ . This is the mean field limit with energy  $E = V_0 M_B \nu_B^2$ .

For finite range interactions terms will remain in the Hamiltonian that connect different orbitals. These will be denoted

$$T = H - H_0. \quad (10)$$

$T$  contains hopping terms between nearest neighbors as the Hubbard Hamiltonian but also contains hopping terms to any neighbor state  $n$ . As the wave functions are rapidly oscillating as described in Appendix A and not in phase in  $T$ , their overlap is generally smaller as those in  $H_0$ . We shall in section V discuss the effect of the hopping terms in  $T$  and possible Mott-Hubbard transitions if  $T$  is strong.

As the direct and exchange potentials depend only on the distance  $n = j - i$  between the two interacting particle sites, we can rewrite the couplings in  $H_0$  as

$$U_n = \frac{1}{2} (V_{ij,ij} + V_{ij,ji}). \quad (11)$$

Note that  $U_{M_B-n} = U_n$ . In the following this double counting is avoided by truncating  $n \leq M_B/2$  and multiplying by a factor of two.

In the following only  $U_n$  will be important whereas the details of the localized wave function and the two-body interaction are contained in  $U_n$ . We shall only assume that the two-body interactions are repulsive and decreasing with range as is the case for Coulomb repulsion between electrons. As result the resulting couplings  $U_n$  will also be repulsive and decreasing functions of the neighbor distance, i.e.  $U_n > U_{n+1} \geq 0$ .

Fortunately, as will be shown in the following section, the Hamiltonian  $H_0$  can be solved for rather general couplings  $U_n$  and a number of qualitative results can be drawn such as incompressible states at fractional fillings. Whether  $H_0$  is a good approximation for the FQHE Hamiltonian  $H$  as argued above will depend on the effect of  $T = H - H_0$  on the ground state as will discussed in section V.

### III. THE GROUND STATE OF THE EBHM IN THE STRONGLY INTERACTING LIMIT

Eqs. (9) and (11) result in a 1D Bose-Hubbard Hamiltonian in the strongly interacting limit extended with far-neighbor interactions  $U_n$  but without hopping terms

$$H_0 = \sum_{i=0}^{M_B-1} \sum_{n \geq 0}^{M_B/2} U_n n_i [n_{i+n} - \delta_{n,0}]. \quad (12)$$

The EBHM also describes optical lattices and reduces to  $H_0$  for strong lattices in the strongly interacting limit near Feshbach resonances [11, 12].

The Bose-Hubbard model has only on-site interactions, i.e. only  $U_0$  is non-zero. The Ising [6] spin model ( $\sigma_i = n_i - 1/2$ ) has only nearest neighbor interaction, i.e. only  $U_1$  is non-zero. A model including next-nearest neighbor

interactions, i.e.  $U_2 \neq 0$  was solved by Stephenson [8] and Majumdar & Gosh [9]. These statistical models mostly investigate phase transitions and critical exponents in one or more dimensions for fixed chemical potential. We are here interested in the ground state (zero temperature) in one dimension in the thermodynamic limit  $N, M_B \rightarrow \infty$  for constant density or filling fraction  $\nu_B = N/M_B$ .

We shall investigate a general class of EBHM with strong repulsive interactions, i.e. Hamiltonians  $H_0$  with repulsive  $U_n \geq 0$ ,  $n = 0, 1, 2, 3$ , etc., that decrease with distance such that  $U_n > U_{n+1}$ , i.e.  $dU_n/dn < 0$ . Eventually we may expect that  $U_n$  becomes negligible at large  $n$  as compared to other effects from impurities, finite temperature or the experimental resolution. In addition, we shall assume convexity [10]

$$U_{n+1} + U_{n-1} - 2U_n > 0, \quad (13)$$

i.e.  $d^2U_n/dn^2 > 0$ .

The ground state is then organized as to minimize its energy. This is achieved by distributing the particles and also vacancies as “evenly” as possible avoiding “clumping”. We shall argue that the particles sites (and vacancies) are ordered with a periodicity or sequences of replicas depending on the filling fraction (see also [10]).

#### A. Fraction of n'th neighbors, $F_n$

As an example, consider the filling fraction 5/9. The ground state is build up of a series of  $M_B/9$  identical sequences (replicas) repeated after each other of the following type

$$\dots | \bullet \bullet \bullet \bullet \bullet \bullet \bullet \bullet \bullet | \bullet \bullet \bullet \bullet \bullet \bullet \bullet \bullet \bullet | \dots \quad \nu_B = 5/9$$

Here:  $\bullet$ =site with a particle and  $\circ$ =hole or vacancy. The delimiter  $|$  separates replicas. Interchanging any  $\bullet$  with a  $\circ$  increases the energy since  $U_n > U_{n+1}$ , and it is therefore the ground state. By translating the whole lattice the nine degenerate ground states are obtained. However, they are not connected by any two-body interactions.

This principle of “evenly ordering” generalizes to any rational number for the filling fraction  $N/M_B = q/n$ . i.e.  $q$  particles in  $n$  states. If  $q \leq n$  there will be  $(n - q)$  vacancies. The minimum energy state is when the  $q$  particles (or  $n - q$  vacancies) are as distributed over the  $n$  sites avoiding clumping.

In the thermodynamic limit  $N, M_B \rightarrow \infty$  it is now a matter of combinatorics to add up the number of  $n$ 'th neighbors. The ground state energy is necessarily a linear function of the couplings  $U_n$

$$E(N/M_B) = M_B \sum_{n=0}^{M_B/2} F_n(\nu_B) U_n. \quad (14)$$

The coefficients  $F_n(\nu_B)$  are functions of the filling fraction. They are the fractions of sites occupied with an

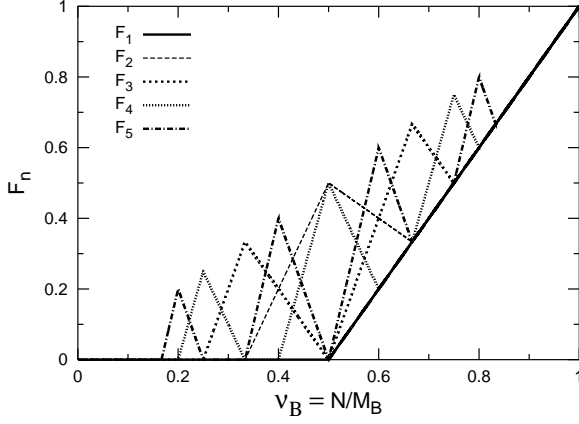


FIG. 1: The fraction of occupied sites with a neighbor  $n$  sites away,  $F_n(\nu_B)$ , for  $n = 1, 2, 3, 4, 5$ .

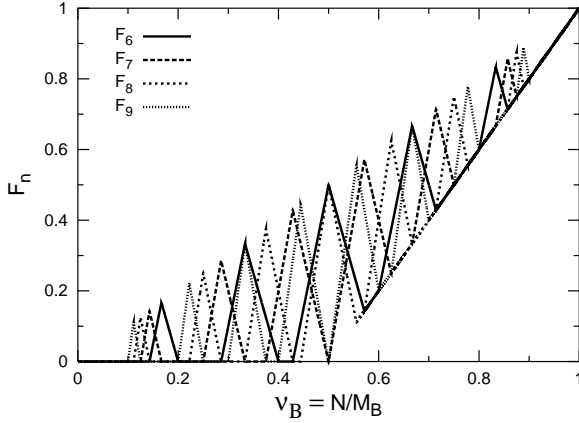


FIG. 2: As Fig. 1 but for  $n = 6, 7, 8, 9$ .

occupation also  $n$  sites to one side (not to both sides in order to avoid double counting). In other words  $M_B F_n(\nu_B)$  is the number of sites occupied which also has a particle displaced  $n$  sites to one side (only to one side when the  $n$  and  $M_B - n$  double counting is avoided). This fraction is necessarily smaller than the filling fraction,  $F_n(\nu_B) \leq \nu_B$ . The ratio  $F_n(\nu_B)/\nu_B$  is the conditional probability for an occupied site to have a neighbor occupation  $n$  sites to one side.

TABLE I: The coefficients in  $F_n = \alpha_n \nu_B + \beta_n$

$\alpha_n$	$\beta_n$	range of $\nu_B$ for $q = 0, 1, \dots, [n/2]$
0	0	$[q/(n-1), (q+1)/(n+1)]$
$1+n$	$-q$	$[q/(n+1), q/n]$
$1-n$	$q$	$[q/n, q/(n-1)]$
$\alpha_n$	$\beta_n$	range of $\nu_B$ for $q = n-1, n-2, \dots, [n/2]$
$1+n$	$-q$	$[(q-1)/(n-1), q/n]$
$1-n$	$q$	$[q/n, (q+1)/(n+1)]$
2	-1	$[q/(n+1), (q+1)/(n+1)]$

It will be shown below that the functions  $F_n$  are piecewise linear functions of  $\nu_B$  (see also Figs. 1+2)

$$F_n = \alpha_n \nu_B + \beta_n. \quad (15)$$

The prefactors  $\alpha_n$  and  $\beta_n$  are discontinuous at the fractions but constant between. They are in fact simple integers of changing signs at the fractions  $\nu_B = q/n$ ,  $q = 1, 2, \dots, n-1$ .

Before deriving their general dependence on  $\nu_B$  analytically a few examples illustrates the general idea. At half filling the state is

$$\dots |\bullet \circ | \bullet \circ | \bullet \circ | \bullet \circ | \bullet \circ | \bullet \circ | \bullet \circ | \bullet \circ | \dots \quad \nu_B = 1/2$$

This is the charge density wave phase of crystalline order at half integer density. This incompressible Mott insulator state also undergoes a transition to a superfluid at a certain hopping strength [17, 18, 19].

Its energy is from Eq. (14)

$$E(1/2) = N \sum_{n=2,4,6,\dots} U_n, \quad (16)$$

i.e.,  $F_n = 0$  for odd  $n$  and  $F_n = 1/2$  for even  $n$ .

Let us next study  $F_1$  and  $F_2$  with increasing filling. The fraction of occupied neighbor states,  $F_1$ , is zero up to half filling,  $\nu_B \lesssim 1/2$ . Above it increases linearly as  $F_1 = 2\nu_B - 1$  reaching unity at full filling  $\nu_B = 1$ . The fraction of next-nearest neighbors is zero for  $\nu_B \lesssim 1/3$  and then increase linearly as  $F_2 = 3\nu_B - 1$  up to half filling, where after it decreases linearly as  $F_2 = 1 - \nu_B$  up to  $\nu_B = 2/3$ .

$$\dots |\bullet \bullet \circ | \bullet \bullet \circ | \bullet \bullet \circ | \bullet \bullet \circ | \bullet \bullet \circ | \bullet \bullet \circ | \bullet \bullet \circ | \dots \quad \nu_B = 2/3$$

For filling above  $\nu_B \geq 2/3$  the number of next-nearest neighbors again increase as  $F_2 = 2\nu_B - 1$  just as  $F_1$ .

The ordering principle implied by the condition  $U_{n+1} < U_n$  allows us to calculate the probability coefficients  $F_n$  generally. Let us start at low filling fraction. For  $\nu_B < 1/(n+1)$  there are no  $n$ 'th neighbors and  $F_n = 0$ . The coefficient now increase linearly up to  $\nu_B = 1/n$  where every particle has an  $n$ 'th neighbor and therefore  $F_n = \nu_B = 1/n$ . By increasing the filling fraction further the number of  $n$ 'th neighbors decrease linearly and in fact vanish again at  $\nu_B = 1/(n-1)$ .  $F_n$  now remains zero from  $\nu_B = 1/(n-1)$  up to  $\nu_B = 2/(n+1)$  where the zig-zag behavior repeats. At  $\nu_B = 2/n$  every particle again has a neighbor  $n$  sites away (and also one in between at  $n/2$  for even  $n$  and at  $(n \pm 1)/2$  for odd  $n$ ). Therefore  $F_n(\nu_B) = \nu_B = 2/n$ .

This zig-zag behavior of  $F_n$  in fact repeats itself around each  $\nu_B = q/n$ ,  $q = 1, 2, \dots, n-1$  (see table 1 and Appendix B) with the same  $\alpha_n$  and  $\beta_n$ . Above  $\nu_B \geq 1/2$ , however, with  $F_n = 2\nu_B - 1$  between the zig-zag's instead of zero.

Because  $F_n$  is piecewise linear between these fractions the coefficients can be calculated directly using that

$F_n(q/n) = q/n$  for  $\nu_B \leq 1/2$  and  $\nu_B \geq 1/2$  respectively. The coefficients are (see also Table 1)

$$\begin{aligned}\alpha_n &= 1 \pm n \\ \beta_n &= \mp q\end{aligned}, \quad (17)$$

in the intervals  $[q/n; q/(n \pm 1)]$ . Between these intervals  $\nu_B \in [q/(n-1), (q+1)/(n+1)]$  they both vanish for  $\nu_B \leq 1/2$ .

For  $1/2 \leq \nu_B \leq 1$  we find the very same coefficients just below and above  $q/n$  as in Eq. (17). However, the range is different (see Table 1) and between these intervals  $F_n = 2\nu_B - 1$ , i.e.  $\alpha_n = 2, \beta_n = -1$ . The coefficients are also shown in Figs. 1+2 for  $n = 1, 2, \dots, 9$ .

For larger filling fractions,  $\nu_B \geq 1$ , the coefficients can be related as

$$F_n(\nu_B) = F_n(\nu_B - 1) + (2\nu_B - 1), \quad (18)$$

i.e., the zig-zag behavior repeats for all  $F_n$  at  $\nu_B = 1 + q/n$ . Note that  $F_0$  vanishes for  $\nu_B \leq 1$  but increases linearly as  $F_0 = \nu_B - 1$  with filling fraction  $1 \leq \nu_B \leq 2$ .

### B. Particle-hole symmetry

The coefficients  $F_n$  and resulting energies can be related at  $\nu_B$  and  $1 - \nu_B$  by exploiting particle-hole symmetry. Since  $M_B F_n(\nu_B)$  is the number of particles with a particle  $n$  sites away,  $M_B(\nu_B - F_n(\nu_B))$  is the number of particles with a hole  $n$  sites away. The latter is by particle-hole symmetry also equal to the number of holes with a particle  $n$  sites away, which again is equal to  $M_B(1 - \nu_B - F_n(1 - \nu_B))$ . Here  $M_B(1 - \nu_B)$  is the number of holes and  $M_B F_n(1 - \nu_B)$  the number of holes with a hole  $n$  sites away. Equating the two numbers for the number of particle-hole neighbors  $n$  sites away gives

$$F_n(\nu_B) = F_n(1 - \nu_B) + 2\nu_B - 1. \quad (19)$$

By insertion in Eq. (14) we obtain the relation

$$E(\nu_B) = E(1 - \nu_B) + (2\nu_B - 1)E(1) \quad (20)$$

Here  $E(1) = \sum_{n \geq 1} U_n$  is the energy for  $N = M_B$ .

A similar relation has been derived for the ground state energy of the FQHE also exploiting particle-hole symmetry [23]

$$E(\nu) = E(1 - \nu) + (2\nu - 1)E(1), \quad (21)$$

Although the two relations appear identical, they are not because  $\nu$  and  $\nu_B$  are different. One obvious cause for this difference is the neglect of  $T$  in the EBHM energy of Eq. (20). For  $N \gg M_B$  the tight-binding approximation is poor as many states overlap. Furthermore, the EBHM energy does not take the Laughlin wave function into account when the energy is calculated. This becomes increasingly important for increasing filling fraction  $N \rightarrow M$  because the Laughlin wave function contains  $N$  powers of  $z$  whereas the EBHM wave function only has  $M_B = M - N$  powers of  $z$ . For these reasons the EBHM ground state energies is not applicable to the FQHE for large filling fractions.

### C. Chemical potential gaps and superfluid states

The chemical potential at zero temperature is now

$$\mu = \left( \frac{dE}{dN} \right)_{M_B} = \sum_n \alpha_n U_n. \quad (22)$$

The chemical potential is therefore also constant between the fractions and exhibit plateaus as shown in Figs. 3+4. At the fractions the chemical potential is discontinuous and therefore an insulator - but a conductor between the fractions. A chemical potential gap appears in the spectrum at each fraction  $q/n$ ,

$$\Delta\mu(q/n) = \mu(q/n)_+ - \mu(q/n)_-, \quad (23)$$

where  $\pm$  refers to the right/left side of the incompressible fraction  $q/n$ . The gap can be calculated from the expression (17) for  $\alpha_n$ . For  $1/2 < \nu_B < 1$  we find

$$\begin{aligned}\Delta\mu(q/n) &= n(U_{n-1} - 2U_n + U_{n+1}) \\ &\simeq n \left( \frac{d^2 U_n}{dn^2} \right).\end{aligned} \quad (24)$$

Note that the convexity condition of Eq. (13) insures that the gap is positive and the system therefore stable.

For  $\nu_B < 1/2$  we obtain

$$\begin{aligned}\Delta\mu(q/n) &= (n-2)U_{n-1} - 2U_n + (n+2)U_{n+1} \\ &\simeq n \left( \frac{d^2 U_n}{dn^2} \right) - 4 \left( \frac{dU_n}{dn} \right).\end{aligned} \quad (25)$$

Again the convexity condition and that  $dU_n/dn < 0$  insures that the gap is positive.

If  $q$  and  $n$  have a common divisor as, e.g.  $4/6=2/3$ , then the gaps add up. The convexity condition may therefore be unnecessarily strict for such fractions.

If the couplings decrease as a power law  $U_n \propto n^{-\gamma}$ , then  $\Delta\mu(q/n) = \gamma(\gamma+1)U_n/n$ , and the gaps decrease faster than  $1/n$ . Numerical calculations of a finite number of electrons on a sphere find FQHE gaps that decrease slightly faster than  $1/n$  [25]. The couplings  $U_n \propto \log(M_B/n)$  leads to gaps scaling as  $\sim 1/n$ . The Coulombic interactions and wave functions localized in  $z$  would lead to  $U_n \simeq e^2/l(n + \text{const.})$  as discussed above. The interaction strength may, however, be weakened by layer thickness and effects of disorder [26]. The corresponding gaps would thus scale as  $\sim e/l n^2$  at large  $n$ .

In the FQHE problem the repulsion between electrons is canceled on average by a background field from the positively charged solid. This mean field is, however, inert and can be ignored in calculated the pressure and chemical potential of the quantum fluid. Likewise, the optical lattice acts as an inert background of the atomic gas systems.

### D. Pressure and incompressible states

The pressure  $P = -(dE/dV) = (\mu N - E)/V$  at zero temperature can be calculated by noting that the volume

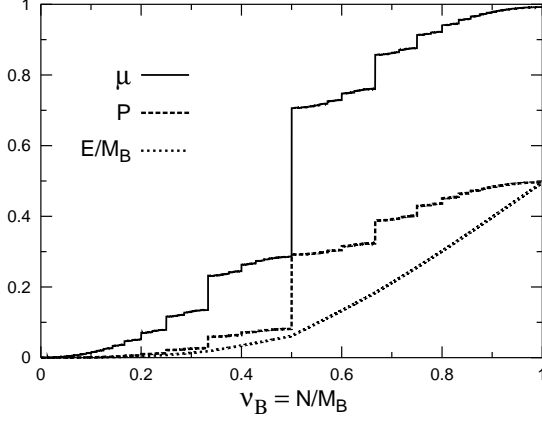


FIG. 3: The energy, chemical potential and pressure vs. filling fraction  $\nu_B$ . A short range two-body interaction is chosen with neighbor couplings  $U_n = 3/(\pi n)^2$ .

is proportional to the number of states  $M_B$  [21]. We shall simply set the volume per state to unity whereby

$$P = - \left( \frac{dE}{dM_B} \right)_N = \mu \nu_B - \frac{E}{M_B} = - \sum_n \beta_n U_n. \quad (26)$$

The pressure is therefore constant, i.e. compressible, between the fractions. If the couplings  $U_n$  are convex we observe that the pressure jumps to a higher pressure and the system is therefore an incompressible quantum fluid at those fractions as shown in Figs. 3+4. If the couplings  $U_n$  are not convex at  $n$ , the pressures may decrease at  $\nu_B = q/n_+$  which would require a Maxwell construction. The pressure discontinuities

$$\Delta P(q/n) = P(q/n_+) - P(q/n_-), \quad (27)$$

can likewise be calculated by inserting the  $\beta_n$  of Eq. (17) in the pressure. For  $\nu_B < 1/2$  we find

$$\begin{aligned} \Delta P(q/n) &= q(U_{n-1} - 2U_n + U_{n+1}) \\ &\simeq q \left( \frac{d^2 U_n}{dn^2} \right), \end{aligned} \quad (28)$$

assuming that  $U_n$  is a smooth function of  $n$ . For  $1/2 < \nu_B < 1$  we find

$$\Delta P(q/n) = (q-1)U_{n-1} - 2qU_n + (q+1)U_{n+1} \quad (29)$$

#### E. Gap dependence on two-body range

In Figs. 3+4 the energy, pressure and chemical potential are shown as function of filling fraction  $\nu_B$  for two representative set of couplings.

The first assumes a short range (delta function) two-body interaction such that the couplings are  $U_n =$

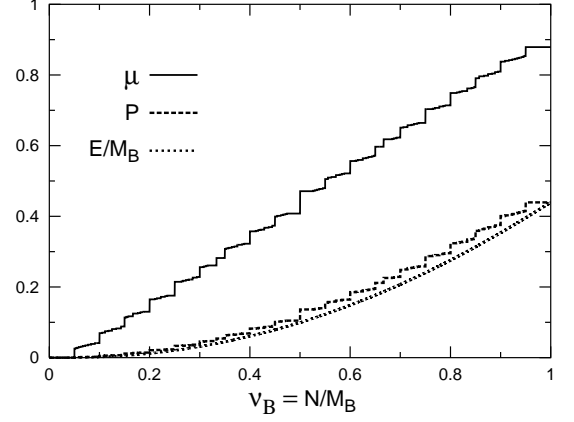


FIG. 4: As Fig. 3 but with neighbor couplings  $U_n = \log(M_B/n)/2M_B$  for  $n \leq M_B = 20$ , which simulates a longer range two-body interaction.

$3/(\pi n)^2$  as discussed above. These couplings decrease rapidly with neighbor distance  $n$  and therefore the chemical potential gaps and pressure discontinuities are largest at the fractions  $q/n$  with small  $n$ , e.g.  $q/n = 1/2, 1/3, 2/3, 1/4, 3/4$ , etc.

In Fig. 4 a longer range two-body interaction is assumed such that the neighbor coupling decrease more slowly with neighbor distance  $n$ . The specific choice is  $U_n = \log(M_B/n)/2M_B$  for  $n \leq M_B = 20$  and vanishing coupling for larger  $n$ . A logarithmic coupling is obtained by averaging a two-body Coulomb potential over radial variables preserving a phase difference  $\phi_1 - \phi_2 = 2\pi n/M_B$ . The rather slow decrease of  $U_n$  with  $n$  has the effect that the gaps and pressure discontinuities only decrease as  $\sim 1/n$ . The long range interaction approaches the mean field limit  $V = V_0$  where  $E/M_B = \nu_B^2/2 = P$  and  $\mu = \nu_B$ .

#### IV. INCOMPRESSIBLE STATES AT FRACTIONAL NUMBERS

The incompressible states found for the system of bosons above can as described in section II be translated to the FQHE states for fermions if we assume that the hopping term  $T$  in the full Hamiltonian is small, or if it does not destroy the incompressible state by making a Mott transition.

The incompressible states in the EBHM appear at fractions  $\nu_B = q/n$ , where  $n$  and  $q$  are integers. However, when applied to the FQHE, it is important first to separate out the Laughlin wavefunction with maximal  $m$  as mentioned in section II. For this reason values  $\nu_B < 1/2$  do not come into play in the FQHE because the preferred ground state wavefunction then includes a Laughlin wavefunction with a  $m$ -value increased by 2.

According to Eq. (4) the Bose fractions correspond to

TABLE II: The leading incompressible filling fractions for small  $n$  and  $q$  for  $m = 1$  (see text). Observed FQHE fractions are given in bold face.

$n$	$q$	$\nu = \nu_B / (1 + m\nu_B) = q / (n + mq)$
1	1,2,3,4,5,6,...	1/2, <b>2/3</b> , 3/4, <b>4/5</b> , 5/6, <b>6/7</b> ,...
2	1,3,5,7,...	<b>1/3</b> , <b>3/5</b> , <b>5/7</b> , 7/9,...
3	2,4,5,...	<b>2/5</b> , <b>4/7</b> , ( <b>5/8</b> ),...
4	3,5,7,...	<b>3/7</b> , <b>5/9</b> , <b>7/11</b> ,...
5	3,4,6,7,..	<b>3/8</b> , <b>4/9</b> , <b>6/11</b> , 7/12, ..
6	5,7,11,...	<b>5/11</b> , <b>7/13</b> , 11/17,...
7	4,5,6,8,...	<b>4/11</b> , ( <b>5/12</b> ), <b>6/13</b> , <b>8/15</b> , ...
8	5,7,9,11,...	<b>5/13</b> , <b>7/15</b> , <b>9/17</b> , 11/19,...
9	5,7,8,10,11,..	( <b>5/14</b> ), 7/16, <b>8/17</b> , <b>10/19</b> , 11/20,...
10	7,9,11,13,..	( <b>7/17</b> ), <b>9/19</b> , <b>11/21</b> , 13/23,...
11	6,7,...	<b>6/17</b> , 7/18,...

FQHE filling fractions

$$\nu = \frac{\nu_B}{1 + m\nu_B} = \frac{q}{n + mq}, \quad (30)$$

where  $m = 1, 3, 5, \dots$  is the Laughlin number. Most of the leading fractions are shown in Table II and will now be compared to the FQHE fractions found in FQHE experiments [2, 3].

#### A. The Laughlin and Jain sequences

The incompressible states at  $\nu_B = 1/2$  gives the Laughlin fractions 1, 1/3, 1/5, 1/7, etc. for  $m = 1, 3, 5, 7, \dots$  respectively. Next to these the most important set of fractions is the Jain sequence

$$\nu = \frac{n}{2n \pm 1}. \quad (31)$$

These appear for  $m = 1$ . Inserting the EBHM fractions  $\nu_B = 1 - 1/n$ ,  $n = 1, 2, 3, \dots$  in Eq. (4) gives the positive (+) part of the principal FQHE fractions, i.e. 1/3, 2/5, 3/7, etc. There are analogous incompressible states at fillings  $\nu_B = 1 + 1/n$ . Inserting these in Eq. (4) they lead to the other (-) half of the principal fractions of Eq. (31), i.e. 2/3, 3/5, 4/7, etc.

The Jain fractions will be leading for two reasons. Firstly, the pressure discontinuity of Eq. (28) increase with  $q$  and  $q = n - 1$  is maximal for these fractions for a given  $n$ . Secondly, in the region above  $\nu_B = 1 - 1/(n - 1)$ , the fraction  $\nu_B = 1 - 1/n$  will be the incompressible fraction with the smallest  $n$ . As the pressure discontinuity of Eq. (28) also decreases with  $n$  it will therefore be the largest in this region.

#### B. $\nu < 1/3$

It was discussed in section II that for fractions  $\nu < 1/m$ ,  $m = 1, 3, 5, \dots$  the Laughlin wave function with  $m$

should be employed. For example, for  $1/5 < \nu < 1/3$  (corresponding to  $1/4 < \nu_B < 1/2$  for  $m = 1$ ) the Laughlin wave function with  $m = 3$  should be employed instead with a larger  $\nu_B$  such that  $\nu = \nu_B / (3\nu_B + 1)$ .

For  $m = 3$  the commensurable fillings  $\nu_B = n$ ,  $n = 2, 3, 4, 5, \dots$ , therefore lead to the fractions 2/7, 3/10, 4/13, 5/16, etc. These first three are clearly identified in the FQHE spectrum [3]. The next leading fractions  $\nu_B = 3/2, 5/2, 7/2$ , etc. gives  $\nu = 2/9, 5/17, 7/23$ , etc., respectively. The two first are also observed in the FQHE spectrum. The large  $\nu_B$  become gradually more difficult to observe because the corresponding FQHE fraction approaches 1/3 and is therefore quenched by the Laughlin fraction  $\nu = 1/3$ .

#### C. $1/3 < \nu < 1/2$

Secondary incompressible states also appear in the EBHM at the fractions  $q/n$ ,  $q = n - 2, n - 3, \dots$ , etc. As their gap size decrease with  $n$  their importance are ordered likewise (see Table II). The leading secondary fractions (not including the Laughlin and Jain series) are therefore:  $\nu_B = 3/5, 4/7, 5/7, 5/8, 5/9, 7/9, 7/10, 6/11$ , etc. These EBHM fractions correspond to the FQHE fractions  $\nu = 3/8, 4/11, 5/12, 5/13, 5/14, 7/16, 7/17, 6/17$ , etc. (see also table II). Remarkably, four of these fractions are clearly identified in recent high resolution FQHE experiments [3]. The fraction at 5/12 is compatible with the structure reported between the principle fractions  $\nu = 2/5$  and 3/7. The fractions 5/14 and 7/17 are compatible with structures between 4/11 and 6/17. The remaining fraction 7/16 is squeezed between the two Jain fractions 3/7 and 4/9 and thus difficult to observe.

Incompressible states with fractions  $q/n$  with larger  $n$  will be weaker. Except for the Jain fractions, they will also be placed between stronger incompressible states, i.e. fractions with smaller  $n$ . Therefore they will be increasingly difficult to identify experimentally. The incompressibilities and chemical potential gaps become smaller and eventually disappear with increasing  $n$ . Effects of impurities, finite temperature and experimental resolution therefore exclude experimental observation of the incompressible states at large  $n$ .

#### D. $\nu = 1/2$

The EBHM is apparently successful in producing all the incompressible states at the principle and secondary FQHE fractions including those found in recent experiments. However, it clearly fails for  $m = 1$  at half filling or  $\nu_B = 1$  where it also predicts an incompressible state in contradiction with FQHE experiments and theoretical calculations [24]. In the Bose-Hubbard model the state at  $N = M_B$  becomes compressible for a sufficiently strong hopping term. It will be discussed in the next section that the hopping term  $T$  may cause a transition from

a Mott insulator to a superconductor, i.e. changes the state at  $\nu = 1/2$  to a compressible one.

### E. $\nu > 1/2$

For  $\nu_B \geq 1$  the EBHM predicts a number of incompressible states. The leading ones are shown in Table II. Experimentally, they are increasingly difficult to observe as  $\nu \rightarrow 1$  due to limited resolution. The set of states at  $\nu_B = 2 - 1/n = 5/3, 7/4, 9/5$ , etc., correspond to FQHE states  $\nu = 5/8, 7/11, 9/14$ , respectively. The  $7/11$  is clearly observed whereas a structure is found at  $5/8$  and possibly also at  $9/14$ .

However, as mentioned above the ground state energies of the EBHM become less reliable with increasing filling fraction as a model for the FQHE. When  $\nu_B > 1$  it is therefore a better approximation to use the particle-hole symmetry of the FQHE, Eq. (21) by inserting the EBHM energies for  $\nu_B < 1$  as an approximation for the FQHE ground state energies. It follows that the incompressible states for  $\nu$  also exist for  $1 - \nu$ .

## V. MOTT-HUBBARD TRANSITIONS

The term  $T$  contains a number of hopping terms between  $n$ 'th neighbors. It is therefore instructive to compare to the one dimensional Bose-Hubbard model (Eq. (1) which contains nearest neighbor hopping  $t_1$  but only on-site interactions, i.e. only  $U_0$  is non-vanishing. In the strongly interacting limit ( $T \ll H_0$ ) it is a Mott insulator for integer filling factors [11, 12] as also found above for the EBHM. Increasing the hopping term a Mott transition takes place at  $t_1 \simeq U_0/1.92$  in one dimension and the system becomes a superfluid.

It is known from studies of the FQHE state at half filling (or  $N/M_B = 1$ ) [24] that the state is compressible. We should therefore expect that by including  $T$  the incompressible state at  $N = M_B$  undergoes a Mott transition.

Adding terms  $U_n \neq 0$  but keeping  $T = 0$ , creates new Mott insulator states at the corresponding fractional filling factors as described above. A crucial question is therefore whether these Mott insulator states survive as the hopping term  $T$  is gradually turned on. Studies of the Bose-Hubbard model including next neighbor interactions show that the Mott insulator state at half filling or charge density wave disappear before that at unity filling as the nearest neighbor hopping  $t_1$  is increased.  $T$  is, however, very different from  $t_1$ .

A closer look at the ground states for fractional and integer filling fractions reveals a difference in the overlap between the degenerate ground states. The ground state for  $N = M_B - 1$

is  $M_B$ -fold degenerate and the hopping term  $T$  couples them all. As a consequence the energy can change considerably. It is the far-neighbor hopping terms in  $T$  that can be responsible for “destabilizing” the integer filling fraction states. Only the nearest neighbor hopping  $t_1$  is present in the Bose-Hubbard model.

In comparison the states near fractional filling, e.g.  $N = 2M_B/3 - 1$

$$...|\bullet\bullet\circ|\bullet\bullet\circ|\bullet\bullet\circ|\bullet\circ\bullet\circ|\bullet\bullet\circ|\bullet\bullet\circ|\bullet\bullet\circ|\bullet\bullet\circ|....$$

this state only couple to two of the  $N$  degenerate ground states, namely those where the extra hole hops one site to one side, resulting in a modest energy corrections.

Another difference appears when comparing the corrections to the ground state energies just above and below  $N/M_B = 2/3$  with those at  $N = M_B$ . In the former case the correction from including hopping terms from  $T$  is the same for  $N = 2M_B/3 \pm 1$ . However, the leading hopping term correction for  $N = M_B \pm 1$  differs because it vanishes when one particle is added to commensurate filling.

It should be noted that only the odd commensurate states  $\nu_B = 1, 3, 5, \dots$  should undergo a Mott transition and only for  $m = 1$  in order to fully agree with the FQHE. It has been argued that the far hopping terms are important for commensurate states but at present the EBHM cannot explain why only the odd commensurate states for  $m = 1$  vanish for the FQHE. It may be related to the difference in energy between the energies of the EBHM and FQHE, Eqs. (19) and (20) respectively. The Laughlin wavefunction may affect energies of the FQHE especially at large filling  $\nu_B$  and  $m$ .

The EBHM is at most an approximation to the FQHE since the localized states are only a good approximation when the hopping terms are small. Furthermore, a bosonization procedure was applied without including the Laughlin wave function, when energies were calculated within the EBHM. These approximations should be investigated further.

The effects of far-neighbor hopping is a complicated yet important problem. Experimentally, it may be studied by quantum gases in optical lattices where the neighbor couplings and hopping can be controlled by tuning the lattice spacing and height, interaction strengths and particle density. Both the neighbor couplings  $U_n$  and the hopping coefficients  $t_n$  decrease exponentially with the tunneling factor  $\sim \exp(-2n\sqrt{V_0/E_R})$ , where  $V_0$  is the optical lattice amplitude and  $E_R$  the recoil energy [12]. In addition, however, the couplings  $U_n$  also scale with the scattering length which allows us to enhance the couplings near a Feshbach resonance and thus reach the strongly interacting limit. If absorption images can be obtained from such a one dimensional optical lattice then Bragg peaks should be observed displaying fractional reciprocal lattice vectors due to the periodicity at fractional filling.

$$.....\bullet\bullet\bullet\bullet\bullet\bullet\bullet\bullet\circ\bullet\bullet\bullet\bullet\bullet\bullet\bullet\bullet\bullet.....$$



## VI. SUMMARY AND OUTLOOK

The Bose-Hubbard model extended by including nearest and far neighbor interactions was related to the fractional quantum Hall effect problem. The ground state is calculated for the extended Bose-Hubbard model in the strongly repulsive limit (weak hopping). Incompressible Mott insulator states were found at filling fractions compatible with the FQHE filling fractions of the lowest Landau level. The incompressible states with the largest gaps are the Laughlin and Jain fractions. Secondary incompressible states occur for filling fractions  $3/8$ ,  $4/11$ ,  $5/13$ ,  $6/17$ ,  $2/7$ ,  $3/10$ ,  $4/13$ ,  $5/16$ ,  $2/9$ ,  $5/17$ . Such fractions have been observed in recent FQHE experiments. Weaker states at  $9/14$ ,  $5/12$ ,  $5/14$ , etc. are also predicted and indications of structures at the fractions are reported in recent high resolution FQHE experiments. Furthermore, incompressible states at fractions with even larger denominators are also predicted; the next candidates would be  $7/16$ ,  $7/17$ ,  $7/23$ , etc. However, these states are increasingly difficult to observe and is a challenge to find experimentally.

The EBHM provides an interesting spectrum of incompressible state at fractional fillings. Whether these states survive or undergoes a Mott insulator transition to a superfluid as the hopping terms are included is an important question. It has been indicated that far hopping terms are important for commensurate states  $\nu_B = 1, 2, 3, \dots$  but it is not clear why only the odd ones should undergo a Mott transition. The EBHM is at most an approximation to the FQHE since the localized states are only a good approximation when the hopping terms are small. Furthermore, a bosonization procedure was applied without including the Laughlin wave function,

when energies were calculated within the EBHM. These approximations should be investigated further.

In spite of its limitations as a model for the FQHE, the EBHM does provide a ground state wave function in the strongly interacting limit from which incompressible fractions, gaps and incompressibilities can be calculated. Corrections from hopping terms may be estimated perturbatively using this wave function as a starting point. Therefore, the EBHM may provide a useful basis for also calculating a number of transport coefficients such as the longitudinal and transverse Hall resistances as well as their low temperature dependence.

The Mott transitions at fractional fillings between insulator and superfluid phases may generally be studied by experiments with quantum gases in optical lattices. By lowering the lattice heights the overlap between nearest and next-nearest neighbors increase and therefore also  $U_1, U_2, \dots$ , and the corresponding hopping terms [27]. In optical lattices the neighbor couplings and hopping can be controlled by tuning the lattice spacing and height as well as the interaction strengths between atoms and the particle density. Furthermore, Bose and Fermi atoms can be mixed resulting in a multitude of Mott, charge and spin density wave, superfluid and other phases [28, 29].

In high temperature superconductivity (HTc) ordered charge density waves are found in the spin glass phase. These are ordered 1D stripe and 2D checkerboard phases with magic hole doping fractions at  $x = 1/16, 3/32, 1/8, 3/16$  [30]. These phases and their competition with HTc are believed to be described by (extended) 2D Hubbard Hamiltonians and therefore such models are actively investigated. The ordering, Mott insulator phases and transitions in lattices with fermions and/or bosons is an important topic in many fields.

- 
- [1] K. v. Klitzing, G. Dorda, M. Pepper, Phys. Rev. Lett. **45**, 494 (1980)
  - [2] D.C. Tsui, H.L. Stormer, A.C. Gossard, Phys. Rev. Lett. **48**, 1559 (1982). H.L. Stormer, Physica B **177**, 401 (1992). R.R. Du, H.L. Stormer, D.C. Tsui, L.N. Pfeiffer, K.W. West, Phys. Rev. Lett. **70**, 2944 (1993).
  - [3] W. Pan, H.L. Stormer, D.C. Tsui, L.N. Pfeiffer, K.W. Baldwin, K.W. West, Phys. Rev. Lett. **90**, 016801 (2003)
  - [4] R.B. Laughlin, Phys. Rev. Lett. **50**, 1395 (1983)
  - [5] "The Quantum Hall Effect", ed. by R.E. Prange and S.M. Girvin (Springer, Berlin, 1986).
  - [6] E. Ising, Zeit. f. Physik **31**, 253-258 (1925).
  - [7] H.A. Bethe, Zeit. f. Physik **71**, 205 (1931).
  - [8] J. Stephenson, Can. J. Phys. **48**, 1724 (1970).
  - [9] C.K. Majumdar & D.K. Ghosh, J. Math. Phys. **10**, 1388 (1969).
  - [10] J. Hubbard, Phys. Rev. B **17**, 494 (1978).
  - [11] M.P.A. Fischer, P.B. Weichman, G. Grinstein, D.S. Fisher, Phys. Rev. B **40**, 546 (1989). D. Jaksch, C. Bruder, J.I. Cirac, C.W. Gardiner, P. Zoller, Phys. Rev. Lett. **81**, 3108 (1998).
  - [12] W. Zwerger, J. Opt. B **5**, 9 (2003).
  - [13] M. Greiner et al., Nature **419**, 51 (2002).
  - [14] A.S. Sørensen, E. Demler, M.D. Lukin, cond-mat/0405079.
  - [15] N.K. Wilkin and J.M.F. Gunn, Phys. Rev. Lett. **84**, 6 (2000).
  - [16] T.-L. Ho, Phys. Rev. Lett. **87**, 060403 (2001).
  - [17] B. Paredes, P. Fedichev, J.I. Cirac, P. Zoller, Phys. Rev. Lett. **87**, 010402 (2001).
  - [18] P. Niyaz, R.T. Scalettar, C.Y. Fong, and G.G. Batrouni, Phys. Rev. B **44**, 7143 (1991); Phys. Rev. B **50**, 362 (1994).
  - [19] T.D. Kühner and H. Monien, Phys. Rev. B **58**, R14741 (1998). T. D. Kuehner, S. R. White, H. Monien, cond-mat/9906019.
  - [20] J.K. Jain, Phys. Rev. Lett. **63**, 199 (1989).
  - [21] For a sample area  $S$  the number of available states in the lowest Landau level is  $M = S/2\pi l^2$  where  $l = \sqrt{\hbar c/eB}$  is the magnetic length.
  - [22] M.I. Dyakonov, *Recent Trends in Theory of Physical Phenomena in High Magnetic Fields*, I.D. Vagner et al (eds.), pp. 75-88, Kluwer Academic Publishers (2003).
  - [23] See, e.g., A.H. MacDonald, cond-mat/9410047.

- [24] B.I. Halperin, P.A. Lee, N. Read, Phys. Rev. B **47**, 7312 (1993).
- [25] R.H. Morf, N. d'Ambrumenil, S. Das Sarma, Phys. Rev. B **66**, 075408 (2002).
- [26] X. Wan et al., cond-mat/0505530.
- [27] G. Mazzearella, S.M. Giampaolo, F. Illuminati, cond-mat/0509161.
- [28] F. Illuminati and A. Albus, Phys. Rev. Lett. **93**, 090406 (2004).
- [29] D.-W. Wang, M.D. Lukin, E. Demmler, cond-mat/0410494.
- [30] S. Komiya, H-D. Chen, S-C. Zhang, Y. Ando, Phys. Rev. Lett. **94**, 207004 (2005).

## APPENDIX A: LOCALIZED STATES ON A CIRCLE

To motivate the basis of localized wave functions in Eq. (5) we discuss the model of Dyakonov [22], where the FQHE problem is approximated by putting the states on a circle.

The idea behind the circle approximation is to replace the coordinates  $z = re^{i\phi}$  by their phase:  $e^{i\phi}$ , by approximating the radius by its average value:  $\langle |z|^2 \rangle = \langle r^2 \rangle = k + 1$ , in units of the magnetic length. The states now become:  $\psi_k \simeq \exp(ik\phi)$ ,  $k = 0, 1, 2, \dots, M_B - 1$ . The Laughlin wave function is then

$$\Psi_m = A \prod_{i < j} (e^{i\phi_i} - e^{i\phi_j})^m, \quad (\text{A1})$$

with  $m = 1, 3, 5, \dots$  and normalization  $A^2 = (m!/2\pi)^N / (mN)!$ .

The Wannier-type localized functions analogous to (5) are simply

$$\begin{aligned} \Phi_j(\phi) &= \frac{1}{\sqrt{2\pi M_B}} \sum_{k=0}^{M_B-1} e^{ik(\phi - 2\pi j/M_B)} \\ &= \frac{1}{\sqrt{2\pi M_B}} \frac{1 - e^{iM_B\phi}}{1 - e^{i(\phi - 2\pi j/M_B)}}, \end{aligned} \quad (\text{A2})$$

where  $j = 0, 1, \dots, M_B - 1$ . These wave functions are localized in angle  $\phi$  around  $2\pi j/M_B$ . They oscillate rapidly with frequency  $1/M_B$  and amplitude dropping off slowly as  $j^{-1}$ . They are the same function (a phase times  $\sin(M_B x)/\sin(x)$  with  $x = \phi/2 - \pi j/M_B$ ) of the shifted angle  $(\phi - 2\pi j/M_B)$ . The localization sites are relative to each other and can all be shifted by an arbitrary angle. A many-body wave function build of such localized states would therefore rather resemble a strongly correlated liquid than a crystal.

On the circle the  $V_{ij,i'j'}$  are simply

$$\begin{aligned} V_{ij,i'j'} &= \int \Phi_i(\phi_1) \Phi_j(\phi_2) \Phi_{i'}^*(\phi_1) \Phi_{j'}^*(\phi_2) \\ &\quad |\Psi_m(\phi_1, \phi_2, \dots)|^2 V(\phi_1 - \phi_2) d\phi_1 d\phi_2, \end{aligned} \quad (\text{A3})$$

where now the two-body potential  $V(\phi_i - \phi_j)$  depends on the angular distance instead of  $|z_i - z_j|$  as in Eq. (6).

The relative simple localized wave functions allows us to study the overlap integrals in  $V_{ij,i'j'}$ . The localized wave functions are rapidly oscillations and generally out of phase except for the coupling between two sites. As result the direct coupling  $V_{ij,ij}$  and the exchange  $V_{ij,ji}$  are the largest. We therefore expect that the tight binding approximation of Eq. (9), which includes only the direct and exchange interactions, is a good approximation. This is especially the case for long range interactions which approaches the mean field limit. In this limit  $V_{ij,i'j'} = \delta_{i,i'} \delta_{j,j'} \int V(\phi) d\phi$ .

For interactions of range shorter than  $\lesssim 1/M_B$ , the two-body potentials can be approximated by a delta-function interaction:  $V(\phi) \simeq 2\pi V_0 \delta(\phi)$ . The resulting  $U_n$  for the delta function interaction are

$$U_n = 2\pi V_0 \int_0^{2\pi} |\Phi_i(\phi)|^2 |\Phi_{i+n}(\phi)|^2 d\phi. \quad (\text{A4})$$

Here, we have ignored the Laughlin wavefunction but will discuss the effect of the correlation hole below. Note that generally  $\sum_n U_n = M_B \int V(\phi) d\phi$  and for the delta-function interaction  $\sum_n U_n = 2\pi M_B V_0$ . Also  $U_n = U_{M_B-n}$ .

Inserting the wave functions of Eq. (A2) in (A4) yields  $U_0 = (2/3) M_B V_0$  and  $U_n = M_B V_0 [M_B \sin(\pi n/M_B)]^{-2}$  for  $n \geq 1$ . In the thermodynamic limit  $M_B \rightarrow \infty$  the couplings scale as  $U_n = M_B V_0 / (\pi n)^2$ . For longer range interaction the couplings  $U_n$  decrease with  $n$  at a slower rate. For a Coulomb-type potential  $V = e^2/|\phi_1 - \phi_2|$  we obtain  $U_n \sim M_B e^2 / (n + \text{const.})$ , where the constant is of order unity and reflects that  $U_n$  is finite due to the correlation hole in the Laughlin wave function.

The delta-function approximation for the short range interaction should only be employed for the bosonic part of the wave function. As a consequence the direct and exchange interaction energies are the same and leads to a factor two. The delta function interaction should not be employed for the fermionic part of the wave function. The exchange part would then cancel the direct part and lead to vanishing interaction energy as it should for an antisymmetric wave function.

For a longer range potential the exchange and direct parts do not cancel. Also the couplings  $U_n$  will decrease slower with  $n$ . Such an example  $U_n \propto \log(M_B/n)$  is shown in Fig. 4.

Returning to the Coulomb potential in coordinate space  $V = e^2/|z_1 - z_2|$  and the localized wave functions of Eq. (5), the couplings of Eq. (11) with (8) become  $U_n \sim (e^2/\langle r \rangle) \log(M_B/n)$ . These wave functions are, however, only localized in their phases. Therefore the 2-D integration over both radius and angle is different than the 1D integration over angle on the circle. The result is a  $\log(M_B/n)$  instead of  $1/n$  respectively.

It may be advantageous to try to construct a basis of wave functions that are localized both radially and in angle  $\phi$ , i.e. in localized in  $z = re^{i\phi}$ . For a Coulomb potential the couplings will also be approximately Coulombic  $U_n \simeq e^2/l(n + \text{const.})$ . Here, the constant takes into

TABLE III: The coefficients in  $F_n = \alpha_n \nu_B + \beta_n$  for  $n \leq 4$ .

distance n	$\alpha_n$	$\beta_n$	range of $\nu_B$
0	0	0	[ 0 , 1 ]
	1	-1	[ 1 , 2 ]
1	0	0	[ 0 , 1/2 ]
	2	-1	[ 1/2 , 1 ]
2	0	0	[ 0 , 1/3 ]
	3	-1	[ 1/3 , 1/2 ]
	-1	1	[ 1/2 , 2/3 ]
	2	-1	[ 2/3 , 1 ]
3	0	0	[ 0 , 1/4 ]
	4	-2	[ 1/4 , 1/3 ]
	-2	1	[ 1/3 , 1/2 ]
	4	-2	[ 1/2 , 2/3 ]
	-2	2	[ 2/3 , 3/4 ]
	2	-1	[ 3/4 , 1 ]
4	0	0	[ 0 , 1/5 ]
	5	-1	[ 1/5 , 1/4 ]
	-3	1	[ 1/4 , 1/3 ]
	0	0	[ 1/3 , 2/5 ]
	5	-2	[ 2/5 , 1/2 ]
	-3	2	[ 1/2 , 3/5 ]
	2	-1	[ 3/5 , 2/3 ]
	5	-3	[ 2/3 , 3/4 ]
	-3	3	[ 3/4 , 4/5 ]
	2	-1	[ 4/5 , 1 ]

account that the coupling  $U_0$  is finite according to definitions in Eq. (8).

## APPENDIX B: TABLES OF $F_n$ COEFFICIENTS

The first coefficients  $F_n = \alpha_n \nu_B + \beta_n$  are listed in Tables III+IV for filling fractions  $\nu_B \leq 1$  and  $n \leq 7$ .

TABLE IV: The coefficients in  $F_n = \alpha_n \nu_B + \beta_n$  for  $n = 5, 6, 7$  in the interval of fractions  $1/2 \leq \nu_B \leq 1$ .

n	$\alpha_n$	$\beta_n$	range of $\nu_B$
5	6	-3	$[1/2, 3/5]$
	-4	3	$[3/5, 2/3]$
	2	-1	$[2/3, 3/4]$
	6	-4	$[3/4, 4/5]$
	-4	4	$[4/5, 5/5]$
	2	-1	$[5/6, 1]$
6	-5	3	$[1/2, 4/7]$
	2	-1	$[4/7, 3/5]$
	7	-4	$[3/5, 2/3]$
	-5	4	$[2/3, 5/7]$
	2	-1	$[5/7, 4/5]$
	7	-5	$[4/5, 5/6]$
	-5	5	$[5/6, 6/7]$
	2	-1	$[6/7, 1]$
7	8	-4	$[1/2, 4/7]$
	-6	4	$[4/7, 5/8]$
	2	-1	$[5/8, 2/3]$
	8	-5	$[2/3, 5/7]$
	-6	5	$[5/7, 3/4]$
	2	-1	$[3/4, 5/6]$
	8	-6	$[5/6, 6/7]$
	-6	6	$[6/7, 7/8]$
	2	-1	$[7/8, 1]$